Journal of Applied Research and Technology

www.jart.icat.unam.mx

Journal of Applied Research and Technology 23 (2025) 22-32

Original

Adsorption of Congo red textile dye on pineapple activated charcoal

M. L. G. Santos[a] • E. C. S. Paz[a] • E. M. Silva[a] • M. M. Pedroza[a]* • L. R. A. Oliveira[b]

[a]*Department of Environmental Engineering, Federal Institute of Tocantins (IFTO)*
[b]*Department of Environmental Technology, University of Ribeirão Preto (UNAERP)*

Received 03 03 2024; accepted 09 10 2024
Available 02 28 2025

Abstract: The work produced activated carbon (CACCA) from the lignocellulosic biomass of pineapple peel and crown (CCA) by slow pyrolysis in a fixed bed reactor. Activation was carried out by water vapor at a temperature of 700 °C for a period of 30 min. The objective was to remove the Congo red textile dye from the charcoal obtained. The biomass showed values for density 0.264 g/ mL, moisture 7.03%, volatile matter 80.74%, ash 6.33%, fixed carbon 5.9%, carbon 43.43%, hydrogen 1.16%, oxygen 48.19%, nitrogen 6.22%. The CACCA yield was 25.24%. CACCA was used in the adsorption process to remove the anionic Congo red dye, using a Plackett-Burman (PB) experimental design. The formation of a mesoporous structure of the activated charcoal and pHpcz of the CACCA favored the adsorption process, which reached up to 94.94% efficiency in the dye removal.

Keywords: Pineapple, pyrolysis, charcoal, adsorption, Plackett-Burman.

*Corresponding author.
E-mail address: mendes@ifto.edu.br (M. M. Pedroza).
Peer Review under the responsibility of Universidad Nacional Autónoma de México.

1. Introduction

Population growth and globalization contribute to the increase in agricultural and industrial waste, which contributes to the collapse of natural resources and water pollution. Therefore, the scientific community has carried out research to minimize the effects of these (Juma et al., 2014). Among The Brazilian industries, textiles represent the largest production chain in the West, which generates a considerable volume of effluents rich in pollutants from the chemical supplies used in the manufacturing process (Pedroza et al., 2021; Popa & Visa, 2017).

Wastewater varies according to its origins. The textile industry uses a variety of products, among which dyes are one of the components used and when in contact with water are harmful to aquatic species (Ahmad et al., 2021; Anjaneyulu et al., 2005; Talouizte et al., 2020).

Dyes are substances that can be classified by their chemical structure, use and/or application in textile fiber. In the textile industry, it is estimated that 100 m^3 of water is used for each ton of fabric processed. To address the impacts caused by wastewater from the dyeing process to the environment, it is necessary to use technologies for the treatment of these effluents (Al-tohamy et al., 2022; Bhatnagar et al., 2015; Khenifi et al., 2007; Khandegar & Saroha, 2013; Yagub et al., 2014).

The textile industry uses dyes that sometimes have complex chemical structures and the removal of these pigments in the aqueous medium can be carried out by different processes, such as oxidative, physical and biological (Juma et al., 2014; Pedroza et al., 2021; Talouizte et al., 2020).

Thus, adsorption with activated carbon has been considered in the removal of dyes in effluents (Fahmy et al., 2020; Lua et al., 2006; Lua., 2020). The charcoal activation process takes place by physical or chemical means to increase the pore surface (Braga et al., 2015). The porous carbonaceous structure of coal, the surface area and its mechanical properties are factors that influence the efficiency of the adsorption process (Braga et al., 2015; Paz et al., 2023; Tang et al., 2019). To produce lignocellulosic activated carbon, raw material is needed in abundance, to be subjected to the thermochemical process, in which its physical and chemical nature is modified in a controlled environment that generates a solid product (Tang et al., 2019).

Brazil is the third world producer of pineapple and part of the crown and bark residues come from the processing industry that can be reused through a thermochemical treatment (Khenifi et al., 2007; Yin et al., 2019). The National Solid Waste Policy (PNRS), Law No. 12305/2010, regulated by Decree No. 10936/2022, deals with a set of principles, objectives, instruments, guidelines, goals and actions that must be taken by government and private entities. The main objectives of the policy are the quality of the environment through non-generation, reduction, recycling, reuse, among other actions, until the proper disposal of tailings (Pedroza et al., 2021; Paz et al., 2023).

Charcoal production from pineapple waste biomass can be an alternative to commercial activated carbon. Therefore, the aim of this research is to produce pyrolytic activated carbon for Congo red dye removal by adsorbing the pollutant using a Plackett-Burman (PB) experimental design.

2. Materials and methods

The material used to carry out this work was the lignocellulosic biomass of the peel and crown of the pineapple (CCA) in the proportion volume/volume of mesh 10, collected in the fairs of Palmas - TO, Brazil. Figure 1 presents the methodological evolution of the procedures performed in the research.

The CCA biomass was inserted into the fixed-bed reactor in a briquette format with dimensions of 32 mm and length of 25 cm, with a mass of approximately 20 g.

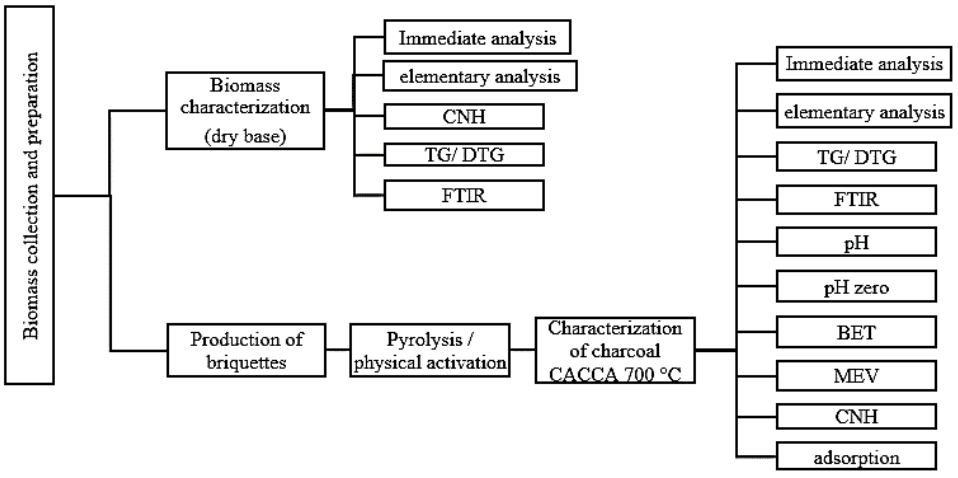

Figure 1. Methodological evolution of research.

To produce coal slow pyrolysis was performed in a stainless-steel fixed bed reactor (Figure 2), with a length of 100 cm and an external diameter of 10 cm, at a temperature of 500 °C, heating rate of 20 °C/min., for a period of 60 min. It was then subjected to a physical activation process with water vapor at a temperature of 700 °C for 30 min to obtain CACCA activated carbon. The steam used during pyrolysis was produced in a vertical autoclave and was directed to the reactor through stainless steel piping at a temperature of 140 °C. After the pyrolysis reactor cooled, the activated carbon was collected directly from the reactor.

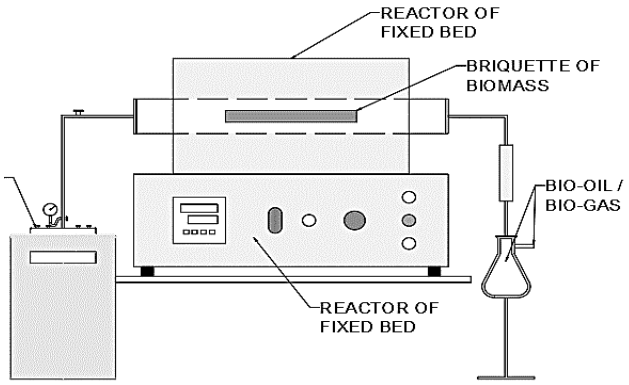

Figure 2. Schematic view of the activated carbon production process from CCA biomass in a fixed bed reactor with activation in water vapor.

The procedures used for the production and characterization of CCA and activated charcoal of pineapple peel and crown (CACCA) are found in Table 1.

Thermogravimetric analysis of the samples were performed using the DSC Q10 - TA instruments, in the temperature range from starting point to 900 °C, with a heating ramp of 10 °C/ min., under a nitrogen atmosphere at a flow rate of 50 mL/ min. FTIR analysis obtained the chemical compounds in the spectrum region in the range of 4000 - 400 cm^{-1} in KBr pellets by Frontier equipment.

CACCA was used in the adsorption process to remove the anionic Congo red dye, using a Plackett-Burman (PB) experimental design to investigate the factors employed in the process, to obtain the removal efficiency and adsorption capacity of the dye (Table 2). In the experimental planning adopted in this research, the following responses were considered: (a) absorbance of the filtrate, (b) dye removal efficiency and (c) adsorption capacity of activated carbon. The adsorption tests were carried out on a bench scale. Plackett-Burman design is generally used in the process of selecting variables or analyzing the effects of factors, in cases where there are more than 5 factors involved, considering the following recommendations: (a) a minimum number of 4 tests more than the number of variables to be studied and (b) carrying out at least 3 tests in the central point condition.

Table 1. Characteristics of the CCA and its CACCA.

Analytical parameter	Analytical method
Density (g/mL)[b]	Gravimetric test
Moisture (%)	ISO-589-1981
Volatile matter (%)[a]	ISO-5623-1974
Ash (%)[a]	ISO-1171-1976
Fixed carbon (%)[a]	By difference
Carbon (%)[b]	Elemental analysis
Hydrogen (%)[b]	Elemental analysis
Oxygen (%)	By difference
Nitrogen (%)[b]	Elemental analysis
Determination of the Zero Load Point	Volumetric analysis
Iodine index (mg/ g)	NBR 11834:1991
Surface area and porosities	Brunauer–Emmett–Teller (BET/JHS/N2)
Thermal characterization	TGA/DTG
Functional groups (%)	FTIR
Micrographs	Scanning Electron electron microscopy (SEM)

[a] Dry basis
[b] Dry and ash free basis

Table 2. Experimental design levels used in the adsorption process of Congo red dye.

Coefficients	Levels		
	(-1)	(0)	(+1)
Temperature (°C)	20	25	30
Congo red concentration (mg/L)	20	40	60
Adsorption time (min.)	10	20	30
Activated carbon mass (g)	0.20	0.50	0.80
Stirring speed (rpm)	71	119	167
Congo red solution pH	6.0	8.0	10

The domains of the effects studied are in accordance with data from the CACCA coal at 700 °C and in accordance with the literature (Paz et al., 2023; Pedroza et al., 2021; Wang et al., 2022).

The lack of degrees of freedom of the PB planning influences the calculation of the standard error, a factor justified by the high reduction in the number of tests and the non-formation of the response surface model (Paz et al., 2023; Pedroza et al., 2021).

3. Results and discussion

3.1. Characterization

The yield of activated carbon produced in the pyrolytic process was 25.24%.

Table 3 shows a value related to the characterization of the residual biomass CCA and CACCA.

Lignocellulosic residues generally have low density, which increases handling, transport and storage costs, thus making their use logistics difficult (Nagarajan & Prakash, 2021; Okot et al., 2019). One of the ways to make the use of biomass viable is to increase the density through briquetting, thus reducing the voids between the particles (Pedroza et al., 2023; Singh et al., 2020).

The Immediate Analysis studies evaluate and determine the physical composition of the residues, being important for the choice of the biomass treatment process. Humidity is one of the factors that influence energy demand and burning, which makes the heat transfer process difficult (Ahmad et al., 202; Pedroza et al., 2023; Talouizte et al., 2020). The number of volatile materials in the biomass represents its conversion into steam and gas after being subjected to the pyrolytic process (Setter et al., 2020). Fixed carbon values are indicative of the calorific value of the briquettes and are associated with the burning speed (Huang & Lo, 2020; Lubwama et al., 2022; Silva et al., 2019). The volatile material and ash contents of the biomass from this research were 80.74 and 6.33%, respectively. The ash content observed in this research was higher than that reported by other researchers when studying coconut fiber (1.98%) and this may be associated with a higher metal content in the pineapple peel and crown (Paz et al., 2023).

The main elemental constituents of the fuel are carbon, hydrogen and oxygen, in addition to relatively low levels of nitrogen (N) and sulfur (S) (Hu & Gholizadeh, 2019). The presence of sulfur was not detected in the biomass sample analyzed in this research, which indicates the use of this residue to produce biofuels.

The charcoal produced in the pyrolytic process stores more stable carbon, explained by the degradation and elimination of volatile materials, cellulose and hemicellulose, with the increase in temperature and reduction of the solid product. The residence time is also responsible for increasing the fixed carbon content because of the release of volatile material (Okot et al., 2019; Pedroza et al., 2023). The lower carbon content of CACCA may be associated with the breakdown of the aromatic structure with increasing temperature.

The volatile values of the CCA biomass justify the reduction in mass and, therefore, in the density of charcoal CACCA. The volatile values of the CACCA are lower than those of the CCA, due to the degradation of lignin and cellulose, which causes an increase in the fixed carbon content.

For solutions with a pH below pHpcz, the adsorbent surface is positively charged and when the pH of the solution is above pHpcz, the adsorbent surface is negatively charged, favoring the adsorption of cationic and anionic dyes, respectively (Paz et al., 2023). Therefore, it is possible to observe that the adsorption can present better results when the solution is negatively charged due to the electrostatic interaction between the adsorbate and the adsorbent CACCA. The effect of pH can be observed in adsorption as it determines the degree of distribution of chemical species. The intensity of this effect may be greater or lesser depending on the adsorbent, since the charges on the surface of the adsorbent depend on its composition and surface characteristics (Ahmad et al., 2021). Figure 3 presents the CACCA pHpcz value.

Table 3. Characteristics of the CCA and CACCA.

Analytical parameter		Values	
		CCA	CACCA
Gravimetric test (g/mL)	Density	0.264	0.107
Immediate Analysis (%)	Moisture	7.03	7.88
	Volatile matter	80.74	32.93
	Ash	6.33	26.83
	Fixed carbon	5.9	32.34
Elementary Analysis (%)	Carbon	43.43	56.94
	Hydrogen	1.16	1.35
	Oxygen	48.19	39.88
	Nitrogen	6.22	1.83
Determination of the Zero Load Point		*	8.00
Iodine index (mg/ g)		*	381.30
Surface area and porosities	Specific surface area (m^2/ g)	*	496.00
	Pore volume (cm^3/ g)	*	0.804
	Pore size (nm)	*	2.39

* Unanalyzed data

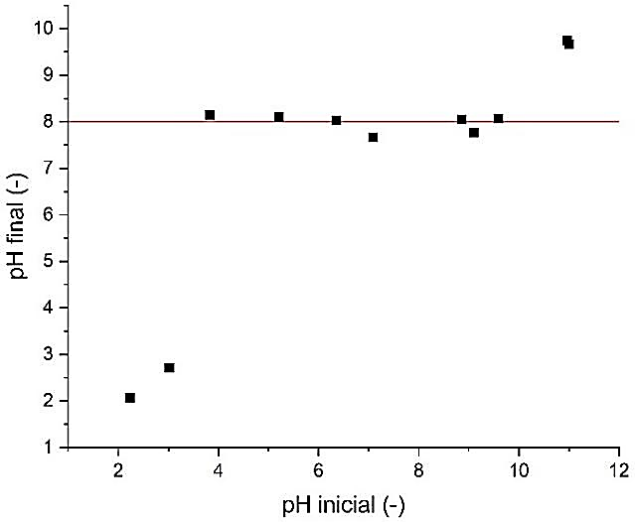

Figure 3. pHpcz CACCA.

The isoelectric point (pHPCZ) of a molecule is the pH at which it is electrically neutral, with the same number of positive and negative charges. The total charge of a molecule depends on the charges of the functional groups that compose it, influenced by their pKa values and the pH of the medium. Figure 3 shows that at a pH lower than 8, activated carbon will be positively charged. Therefore, for the best electrostatic attraction to occur, the dye studied in this research must be negatively charged.

The estimate of microporosity of the pyrolytic charcoal was made through a mathematical relationship, mass of iodine retained per gram of charcoal. CACCA has an adsorption capacity (381.30 mg/g) below the minimum value (600 mg/g) determined by NBR 11834:1991. Therefore, the CACCA charcoal did not present enough micropores; therefore, it did not meet the requirements of the Brazilian standard. Paz et al. (2023) report that pyrolysis temperature can interfere with charcoal quality. The researchers found different iodine index values for activated charcoal obtained from coconut fiber at two temperatures 550 °C (390 mg/g) and 700 °C (536 mg/g).

Elevated temperatures cause an increase in the activated carbon surface, by building new pores and increasing the opening of existing pores. This phenomenon results in the improvement of the adsorption process. CACCA charcoal presented pore diameters in the range of 2 – 50 nm, therefore it is considered mesoporous (Paz et al., 2023; Zolgharnein et al., 2017).

Figures 4 and 5 show thermogravimetric curves (TG) and derivative thermogravimetric (DTB) for CCA and it CACCA. The curves were obtained with the application of heating rates of 10 and 30 °C/ min.

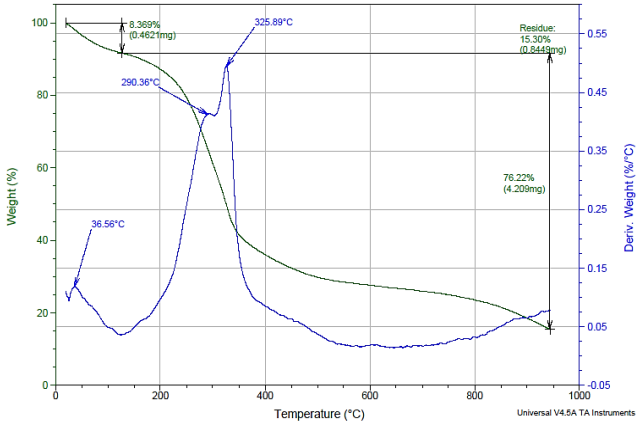

Figure 4. Thermogravimetric degradation curve of the CCA.

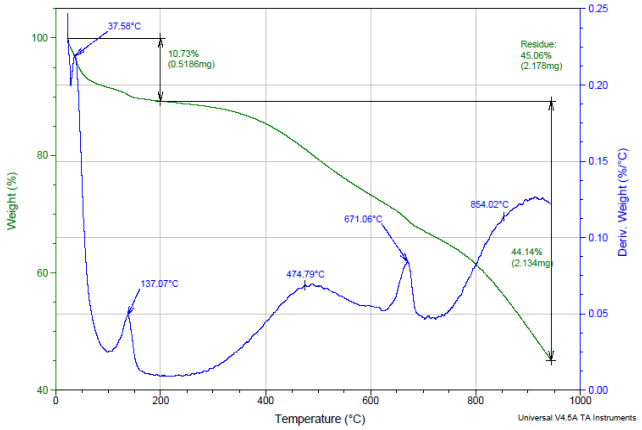

Figure 5. Thermogravimetric degradation curve of the CACCA.

Stage I occurred up to a temperature of 150 °C, with a mass loss of 8.39 % corresponding to moisture and some low molecular weight volatile compounds. The second stage, also known as devolatilization of biomass, occurred between temperatures of 150 to 400 °C, with the elimination of hemicellulose and cellulose and presented a mass loss of almost 50 %. In stage two, it is possible to observe in the DTG the highest peak of biomass degradation at the temperature of 325.89 ° C. The third stage is in the range of 400 to 750 °C, which is characterized by the decomposition of lignin. From a temperature of 750 °C onwards, an inclination can be seen in the curve, which may be characteristic of the breakdown of stable compounds and the formation of ash (Pedroza et al., 2021; Pedroza et al., 2023).

The CACCA thermogravimetric behavior showed up to 200 °C two peaks (37.58 and 137.07 °C) corresponding to the elimination of moisture and in the temperature range from 200 to 900 °C, three peaks were detected at temperatures 474, 671 and 854 °C, with a total mass loss of 44.14%. At 854.02 °C

it is possible that it is indicative of the breakdown of lignin and formation of inorganic compounds.

FTIR analysis was performed to determine the functional groups that absorb radiation at different wavelengths. Figure 6 informs CCA FTIR spectrum and Figure 7 displays spectrum for CACCA in the infrared regions of 4000 – 400 cm^{-1}.

The broad band in the region of 3415.93 cm^{-1} is caused by strain vibrations from the stretching of the O - H functional groups, bonded by hydrogen and water. In the region of 2920.35 cm^{-1}, an asymmetrical elongation of C - H was observed, characteristic of the decomposition of lignocellulosic compounds, mainly cellulose. The 1640.60 cm^{-1} peak is typical of the elongation of the C = C benzene rings present in lignin. The functional groups indicated in the regions 1421.72 and 1381.46 cm^{-1} result from the deformation corresponding to the O - CH elongation attributed to alcohols (fructose) and from the axial deformation of CH, O - H and C - O elongation present in lignin, respectively (Paz et al., 2023; Pedroza et al., 2023).

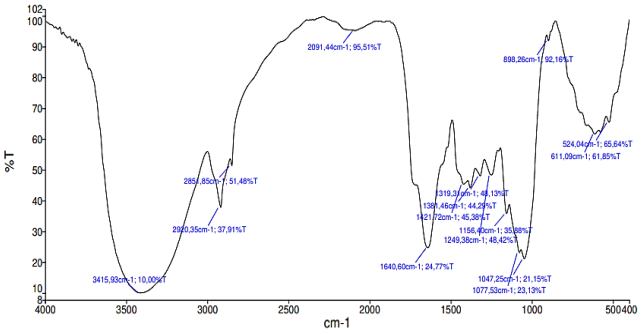

Figure 6. Infrared spectrum of CCA biomass.

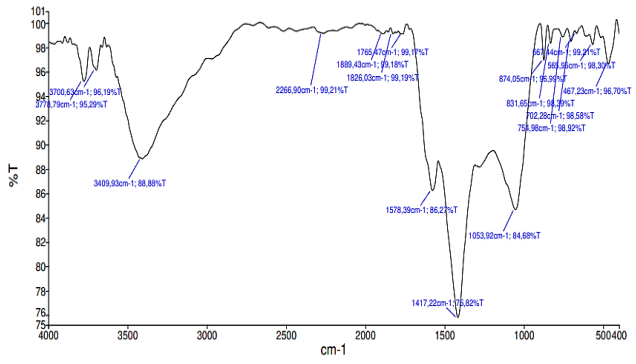

Figure 7. Infrared spectrum of CACCA biomass.

In the region of 3778.89 and 3700.63 cm^{-1} they correspond to axial vibrations that are a result of the bonds in the aromatic and heteroaromatic groups. The 3409.93 cm^{-1} peak is indicative of the presence of the O - H group elongation strain. The functional groups indicated in the regions 1765.47 and 1578.39 cm^{-1} deal with the axial deformation of C = O, referring to the carboxylic acid, acetate, ketone, aldehyde groups. While at 1417.22 cm^{-1} it corresponds to the deformation of O - CH and at 1053.92 cm^{-1} it refers to the stretching of C - O characteristic of alcohol, ethers, esters, carboxylic acids and anhydrides (Biagini et al., 2008; Pedroza et al., 2021; Sengar et al., 2022).

Figure 8 shows a micro image of CACCA with a porous structure in evidence.

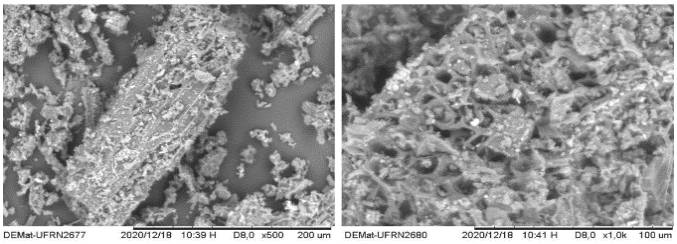

Figure 8. CACCA scanning electron microscopy.

It is possible to see that the CACCA is formed by rough particles with irregular porous surfaces with formation of cavities. The holes formed on the surface of the CACCA are due to the elimination of volatile materials during the pyrolytic process and the presence of microcrystals may be associated with inorganic substances. The structure of activated carbon is influenced by the properties of origin of the biomass, as well as the factors used in the pyrolytic process (Calixto et al., 2022; Fareez et al., 2018; Sekhon et al., 2021; Zolgharnein et al., 2017).

The results obtained in the adsorption process of Congo red anionic dye are shown in Table 4. These were obtained from the factors and levels of experimental design presented in Table 2. The removal efficiency of Congo red dye in the adsorption process ranged from 51.40% to 94.94%. Throughout the process, it is possible to see that the removal capacity of the Congo red dye ranged from 0.59 to 8.14 mg/g. The results of the main effects are presented in Table 5 for absorbance capacity, Table 6 for removal efficiency and Table 7 for adsorption capacity.

The significant effects on adsorption capacity were the concentration of Congo red dye and CACCA activated carbon mass (Table 5).

The factors (operating temperature, Congo red dye concentration, adsorption time, activated carbon mass, stirring speed and Congo red solution pH) were used in the Congo red dye adsorption process in CACCA to obtain the absorbance capacity (Table 5), removal efficiency (Table 6) and adsorption capacity (Table 7) within the 95% confidence interval.

The highest dye removal efficiency by activated carbon was 94.94%, with this experiment being conducted under the following conditions: (a) temperature 30 °C, (b) dye concentration equal to 60 mg/L, (c) adsorption time of 10 min, (d) carbon mass of 0.8 g, (e) stirring speed of 167 rpm and (f)

pH of the dye solution equal to 6. The lowest dye removal efficiency was approximately 50% when the experiment was conducted with the lowest mass of activated carbon (0.2 g) and high pH of the dye solution.

In Table 5, the charcoal mass factor has a negative effect, indicating that the increase in the CACCA charcoal mass reduces the absorptive capacity for the Congo red dye.

For the removal efficiency of Congo red dye, no factor showed significance, however solutions with pH 6.0 and 8.0 showed better interaction between adsorbent and adsorbate, such influence can be confirmed in the analysis of pHpcz, the same occurred in the study conducted by Ponnusamy and Subramaniam (2013). The decrease in efficiency with increasing adsorption rate may be related to the process of adsorbate desorption in the adsorbent. In Table 6, it shows that the factors temperature, stirring speed and pH of the solution negatively interfere in the adsorption process.

Regarding the dye removal efficiency, the effect of the coal mass was positive (16.35), indicating that for greater dye removal a greater amount of adsorbent is required (p-value 0.0149).

The factors adsorbate concentration and adsorbent mass were the ones that showed significance in the process of adsorption capacity of the Congo red dye (Table 7), this influence is inversely proportional. Therefore, when the amount of adsorbent increases and the amount of adsorbate decreases, the adsorption capacity tends to decrease. Temperature has a negative effect on the adsorption process, as it is related to the reduction in the removal capacity of adsorbate (Ponnusamy & Subramaniam, 2013).

The stirring speed did not have a significant effect on the responses adopted in the experimental design (p-value above 0.32) and this indicates that the experiments can be performed at the lowest stirring speed (71 rpm), representing a lower energy expenditure in the adsorption process. No significant difference was observed for the adsorption time factor (p-value above 0.19), indicating that the adsorption experiments can be performed in the shortest time (10 min).

Table 4. Results of experiments used in BP planning - Congo red dye.

Order of Experiments	Coefficient 1 °C	2 mg/L	3 min.	4 g	5 rpm	6 pH	Answers Absorbance capacity (-)	Removal efficiency (%)	Adsorption capacity mg/g
1	30	20	30	0.2	71	6.0	0.13	78.87	2.37
2	30	60	10	0.8	71	6.0	0.09	94.80	2.13
3	20	60	30	0.2	167	6.0	0.18	90.48	8.14
4	30	20	30	0.8	71	10	0.04	91.66	0.69
5	30	60	10	0.8	167	6.0	0.09	94.94	2.14
6	30	60	30	0.2	167	10	0.55	72.66	6.54
7	20	60	30	0.8	71	10	0.13	93.25	2.10
8	20	20	30	0.8	167	6.0	0.14	78.28	0.59
9	20	20	10	0.8	167	10	0.04	92.82	0.70
10	30	20	10	0.2	167	10	0.32	51.40	1.54
11	20	60	10	0.2	71	10	0.51	74.79	6.73
12	20	20	10	0.2	71	6.0	0.13	79.45	2.38
13	25	40	20	0.5	119	8.0	0.08	92.85	2.23
14	25	40	20	0.5	119	8.0	0.10	91.98	2.21
15	25	40	20	0.5	119	8.0	0.11	90.96	2.18

Where the factors are: (1) operating temperature, (2) Congo red dye concentration, (3) adsorption time, (4) activated carbon mass, (5) stirring speed, and (6) solution pH Congo red.

Table 5. Estimates by point, by interval and hypothesis tests for the effects of absorbance in the process of adsorption of Congo red dye from pyrolytic charcoal CACCA, at 95% confidence interval.

Coefficient	Effect	Standard error	t calculated (5)	p-value
Average	**0.19**	**0.03**	**6.50**	**0.0003**
Curvature	-0.20	0.13	-1.47	0.1846
Temperature (x_1)	0.02	0.06	0.31	0.7639
Congo red concentration (x_2)	0.13	0.06	2.09	0.0748
Adsorption time (x_3)	0.00	0.06	0.00	1.0000
Charcoal mass (x_4)	-0.22	0.06	-3.63	0.0085
Stirring speed (x_5)	0.05	0.06	0.79	0.4574
Congo red solution pH (x_6)	0.14	0.06	2.30	0.0547

Table 6. Estimates by point, by interval and hypothesis tests for the effects of removal efficiency in the adsorption process of Congo red dye from pyrolytic charcoal CACCA, at 95% confidence interval.

Coefficient	Effect	Standard error	t calculated (5)	p-value
Average	**82.78**	**2.55**	**32.46**	**0.0000**
Curvature	18.29	11.40	1.60	0.1527
Temperature (x_1)	-4.13	5.10	-0.81	0.4451
Congo red concentration (x_2)	8.07	5.10	1.58	0.1574
Adsorption time (x_3)	2.83	5.10	0.56	0.5957
Charcoal mass (x_4)	16.35	5.10	3.21	0.0149
Stirring speed (x_5)	-5.37	5.10	-1.05	0.3271
Congo red solution pH (x_6)	-6.71	5.10	-1.032	0.2297

Table 7. Estimates by point, by interval and hypothesis tests for the effects of the adsorption capacity of the Congo red dye, in a 95% confidence interval.

Coefficient	Effect	Standard error	t calculated (5)	p-value
Average	**3.00**	**0.28**	**10.81**	**0.0000**
Curvature	-1.59	1.24	-1.28	0.2404
Temperature (x_1)	-0.87	0.56	-1.57	0.1604
Congo red concentration (x_2)	**3.25**	**0.56**	**5.85**	**0.0006**
Adsorption time (x_3)	0.80	0.56	1.44	0.1933
Charcoal mass (x_4)	**-3.23**	**0.56**	**-5.81**	**0.0007**
Stirring speed (x_5)	0.54	0.56	0.97	0.3629
Congo red solution pH (x_6)	0.09	0.56	0.16	0.8750

4. Conclusions

According to the experimental ones of this research, the following conclusions are presented:

The CCA lignocellulosic biomass presented carbon with lower stability and high value of volatiles, which may be associated with the sugars present in its composition. The increase in temperature contributes to the opening of existing and new pores, corroborating the classification of mesoporosity of the CACCA. Based on the thermogravimetric analysis, the temperature range from 200 to 400 ^{o}C showed the highest degradation of the compounds (hemicellulose and cellulose). CACCA presented pHpcz with basic characteristics which results in an adsorption process when adsorbate is negatively charged due to electrostatic interaction between them.

The FTIR CACCA presented characteristic vibrations indicative of aromatic and heteroaromatic groups, elongation of the O-H group, carboxylic acid, acetate, ketone, aldehyde groups and characteristics of alcohol, ethers, esters, carboxylic acids and anhydrides. In the adsorption process, the best removal efficiency of Congo red dye was with a low amount of adsorbent and with the pH of the solution below CACCA pHpcz. In the adsorption process, the efficiency of Congo red dye removal showed values of up to 94.94%, confirming the values found in the pHpcz and BET analyses, therefore, the process is efficient in removing anionic dyes.

Conflict of interest

The authors do not have any type of conflict of interest to declare.

Acknowledgements

The authors thank the National Council for Scientific and Technological Development (CNPq).

Funding

This manuscript was financially supported by Instituto Federal de Educação, Ciência e Tecnologia do Tocantins (IFTO) (Process: EDITAL N^{o} 28/2021/REI/IFTO).

References

Ahmad, M. A., Yusop, M. F. M., Zakaria, R., Karim, J., Yahaya, N. K. E., Yusoff, M. A. M., ... & Abdullah, N. S. (2021). Adsorption of methylene blue from aqueous solution by peanut shell based activated carbon. *Materials Today: Proceedings*, *47*, 1246-1251. https://doi.org/10.1016/j.matpr.2021.02.789

Al-Tohamy, R., Ali, S. S., Li, F., Okasha, K. M., Mahmoud, Y. A. G., Elsamahy, T., ... & Sun, J. (2022). A critical review on the treatment of dye-containing wastewater: Ecotoxicological and health concerns of textile dyes and possible remediation approaches for environmental safety. *Ecotoxicology and Environmental Safety*, *231*, 113160. https://doi.org/10.1016/j.ecoenv.2021.113160

Anjaneyulu, Y., Sreedhara Chary, N., & Samuel Suman Raj, D. (2005). Decolourization of industrial effluents–available methods and emerging technologies–a review. *Reviews in Environmental Science and Bio/Technology*, *4*, 245-273. https://doi.org/10.1007/s11157-005-1246-z

Bhatnagar, A., Sillanpää, M., & Witek-Krowiak, A. (2015). Agricultural waste peels as versatile biomass for water purification–A review. *Chemical Engineering Journal*, *270*, 244-271. https://doi.org/10.1016/j.cej.2015.01.135

Biagini, E., Narducci, P., & Tognotti, L. (2008). Size and structural characterization of lignin-cellulosic fuels after the rapid devolatilization. *Fuel*, *87*(2), 177-186. https://doi.org/10.1016/j.fuel.2007.04.010

Braga, R. M., Queiroga, T. S., Calixto, G. Q., Almeida, H. N., Melo, D. M. A., Melo, M. A. F., ... & Curbelo, F. D. S. (2015). The energetic characterization of pineapple crown leaves. *Environmental Science and Pollution Research*, *22*, 18987-18993. https://doi.org/10.1007/s11356-015-5082-6

Calixto, G. Q., Melo, D. M., Melo, M. A., & Braga, R. M. (2022). Analytical pyrolysis (Py–GC/MS) of corn stover, bean pod, sugarcane bagasse, and pineapple crown leaves for biorefining. *Brazilian Journal of Chemical Engineering*, 1-10. https://doi.org/10.1007/s43153-021-00099-1

Fahmy, T. Y., Fahmy, Y., Mobarak, F., El-Sakhawy, M., & Abou-Zeid, R. E. (2020). Biomass pyrolysis: past, present, and future. *Environment, Development and Sustainability*, *22*, 17-32. https://doi.org/10.1007/s10668-018-0200-5

Fareez, I. M., Ibrahim, N. A., Wan Yaacob, W. M. H., Mamat Razali, N. A., Jasni, A. H., & Abdul Aziz, F. (2018). Characteristics of cellulose extracted from Josapine pineapple leaf fibre after alkali treatment followed by extensive bleaching. *Cellulose*, *25*, 4407-4421. https://doi.org/10.1007/s10570-018-1878-0

Hu, X., & Gholizadeh, M. (2019). Biomass pyrolysis: A review of the process development and challenges from initial researches up to the commercialisation stage. *Journal of Energy Chemistry*, *39*, 109-143. https://doi.org/10.1016/j.jechem.2019.01.024

Huang, Y. F., & Lo, S. L. (2020). Predicting heating value of lignocellulosic biomass based on elemental analysis. *Energy*, *191*, 116501. https://doi.org/10.1016/j.energy.2019.116501

Juma, D. W., Wang, H., & Li, F. (2014). Impacts of population growth and economic development on water quality of a lake: case study of Lake Victoria Kenya water. *Environmental Science and Pollution Research*, *21*, 5737-5746. https://doi.org/10.1007/s11356-014-2524-5

Khandegar, V., & Saroha, A. K. (2013). Electrocoagulation for the treatment of textile industry effluent–a review. *Journal of environmental management*, *128*, 949-963. https://doi.org/10.1016/j.jenvman.2013.06.043

Khenifi, A., Bouberka, Z., Sekrane, F., Kameche, M., & Derriche, Z. (2007). Adsorption study of an industrial dye by an organic clay. *Adsorption*, *13*(2), 149-158. https://doi.org/10.1007/s10450-007-9016-6

Lua, A. C. (2020). A detailed study of pyrolysis conditions on the production of steam-activated carbon derived from oil-palm shell and its application in phenol adsorption. *Biomass Conversion and Biorefinery*, *10*, 523-533. https://doi.org/10.1007/s13399-019-00447-9

Lua, A. C., Lau, F. Y., & Guo, J. (2006). Influence of pyrolysis conditions on pore development of oil-palm-shell activated carbons. *Journal of analytical and applied pyrolysis*, *76*(1-2), 96-102. https://doi.org/10.1016/j.jaap.2005.08.001

Lubwama, M., Yiga, V. A., & Lubwama, H. N. (2022). Effects and interactions of the agricultural waste residues and binder type on physical properties and calorific values of carbonized briquettes. *Biomass Conversion and Biorefinery*, *12*(11), 4979-4999. https://doi.org/10.1007/s13399-020-01001-8

Nagarajan, J., & Prakash, L. (2021). Preparation and characterization of biomass briquettes using sugarcane bagasse, corncob and rice husk. *Materials Today: Proceedings*, *47*, 4194-4198.
https://doi.org/10.1016/j.matpr.2021.04.457

Okot, D. K., Bilsborrow, P. E., & Phan, A. N. (2019). Briquetting characteristics of bean straw-maize cob blend. *Biomass and Bioenergy*, *126*, 150-158.
https://doi.org/10.1016/j.biombioe.2019.05.009

Paz, E. C. S., Paschoalato, C. F., Arruda, M. G., Silva, G. G., Santos, M. L. G., Pedroza, M. M., & Oliveira, L. R. A. (2023). Production and characterization of the solid product of coconut pyrolysis. *Biomass Conversion and Biorefinery*, *13*(7), 6317-6329.
https://doi.org/10.1007/s13399-021-01561-3

Pedroza, M. M., Machado, P. R. S., Silva, J. G. D., Arruda, M. G., & Picanço, A. P. (2023). Production and application of activated carbon obtained from the thermochemical degradation of corn cob. *Journal of Applied Research and Technology*, *21*(6), 952-964.
https://doi.org/10.22201/icat.24486736e.2023.21.6.2173

Pedroza, M. M., Neves, L. H., Paz, E., Silva, F. M., Rezende, C. S., Colen, A. G., & Arruda, M. G. (2021). Activated charcoal production from tree pruning in the Amazon region of Brazil for the treatment of gray water. *Journal of applied research and technology*, *19*(1), 49-65.
https://doi.org/10.22201/icat.24486736e.2021.19.1.1492

Ponnusamy, S. K., & Subramaniam, R. (2013). Process optimization studies of Congo red dye adsorption onto cashew nut shell using response surface methodology. *International Journal of Industrial Chemistry*, *4*, 1-10.
https://doi.org/10.1186/2228-5547-4-17

Popa, N., & Visa, M. (2017). The synthesis, activation and characterization of charcoal powder for the removal of methylene blue and cadmium from wastewater. *Advanced Powder Technology*, *28*(8), 1866-1876.
https://doi.org/10.1016/j.apt.2017.04.014

Sekhon, S. S., Kaur, P., & Park, J. S. (2021). From coconut shell biomass to oxygen reduction reaction catalyst: Tuning porosity and nitrogen doping. *Renewable and Sustainable Energy Reviews*, *147*, 111173.
https://doi.org/10.1016/j.rser.2021.111173

Sengar, A. S., Sunil, C. K., Rawson, A., & Venkatachalapathy, N. (2022). Identification of volatile compounds, physicochemical and techno-functional properties of pineapple processing waste (PPW). *Journal of Food Measurement and Characterization*, 1-13.
https://doi.org/10.1007/s11694-021-01243-8

Setter, C., Borges, F. A., Cardoso, C. R., Mendes, R. F., & Oliveira, T. J. P. (2020). Energy quality of pellets produced from coffee residue: Characterization of the products obtained via slow pyrolysis. *Industrial Crops and Products*, *154*, 112731.
https://doi.org/10.1016/j.indcrop.2020.112731

Silva, D. A. D., Eloy, E., Caron, B. O., & Trugilho, P. F. (2019). Elemental chemical composition of forest biomass at different ages for energy purposes. *Floresta e Ambiente*, *26*(4), e20160201.
https://doi.org/10.1590/2179-8087.020116

Singh, S., Chakraborty, J. P., & Mondal, M. K. (2020). Torrefaction of woody biomass (Acacia nilotica): Investigation of fuel and flow properties to study its suitability as a good quality solid fuel. *Renewable Energy*, *153*, 711-724.
https://doi.org/10.1016/j.renene.2020.02.037

Talouizte, H., Merzouki, M., Benlemlih, M., & Bendriss Amraoui, M. (2020). Chemical characterization of specific micropollutants from textile industry effluents in Fez City, Morocco. *Journal of Chemistry*, *2020*(1), 3268241.
https://doi.org/10.1155/2020/3268241

Tang, Q., Shi, C., Shi, W., Huang, X., Ye, Y., Jiang, W., ... & Li, D. (2019). Preferable phosphate removal by nano-La (III) hydroxides modified mesoporous rice husk biochars: Role of the host pore structure and point of zero charge. *Science of the Total Environment*, *662*, 511-520.
https://doi.org/10.1016/j.scitotenv.2019.01.159

Wang, Z., Tang, Z., Xie, X., Xi, M., & Zhao, J. (2022). Salt template synthesis of hierarchical porous carbon adsorbents for Congo red removal. *Colloids and Surfaces A: Physicochemical and Engineering Aspects*, *648*, 129278.
https://doi.org/10.1016/j.colsurfa.2022.129278

Yagub, M. T., Sen, T. K., Afroze, S., & Ang, H. M. (2014). Dye and its removal from aqueous solution by adsorption: a review. *Advances in colloid and interface science*, *209*, 172-184.
https://doi.org/10.1016/j.cis.2014.04.002

Yin, Y., Zhou, T., Luo, H., Geng, J., Yu, W., & Jiang, Z. (2019). Adsorption of arsenic by activated charcoal coated zirconium-manganese nanocomposite: performance and mechanism. *Colloids and Surfaces A: Physicochemical and Engineering Aspects*, *575*, 318-328. https://doi.org/10.1016/j.colsurfa.2019.04.093

Zolgharnein, J., Bagtash, M., Feshki, S., Zolgharnein, P., & Hammond, D. (2017). Crossed mixture process design optimization and adsorption characterization of multi-metal (Cu (II), Zn (II) and Ni (II)) removal by modified Buxus sempervirens tree leaves. *Journal of the Taiwan Institute of Chemical Engineers*, *78*, 104-117. https://doi.org/10.1016/j.jtice.2017.03.020